JOURNAL OF CATALYSIS **168,** 471–481 (1997)
ARTICLE NO. CA971646

Infrared Study and Quantum Calculations of the Conversion of Methylbutynol into Hydroxymethylbutanone on Zirconia

F. Audry, P. E. Hoggan, J. Saussey, J. C. Lavalley,[1] H. Lauron-Pernot,[2] and A. M. Le Govic[3]

Laboratoire de Catalyse et Spectrochimie, URA 414, Institut des Sciences de la Matière et de Rayonnement, 6 Bd du Maréchal Juin, 14050 Caen Cedex, France

Received October 23, 1996; revised January 20, 1997; accepted January 20, 1997

The activity and selectivity of metal oxides toward 2-methyl-3-butyn-2-ol (methylbutynol, MBOH) conversion depend on their surface properties. The aim of the present work was to explain the formation of 3-hydroxy-3-methyl-2-butanone (hydroxymethylbutanone, HMB) on zirconia. IR study showed that MBOH and HMB adsorption on ZrO_2 was dissociative with the formation of alcoholate species. The transformation of MBOH toward HMB involved residual surface hydroxyl groups or traces of water either contained in the MBOH reactant or formed from MBOH condensation on residual hydroxyl groups and polymerization of acetone, a by-product of the reaction. This polymerization caused a deactivation of the MBOH hydration. Quantum chemistry calculations indicated that π electrons from the acetylenic MBOH triple bond interacted with a vacant zirconium *d* orbital polarizing this π distribution and hence facilitating nucleophilic attack of the carbon 2 (−C−C≡C−H). This suggested that active sites in the formation of HMB can be acid–base *M*–O sites, in which *M* represents a metal with vacant *d* orbitals. Since the addition of water can noticeably favor HMB formation, it thus appears that the MBOH test should be supported by a systematic study of the effect of adding water to the reactant to evidence possible formation of HMB on the catalyst studied.

INTRODUCTION

The importance of inorganic solid surface acid–base properties in heterogeneous catalysis reactions has given rise to a great deal of research on their characterization. Two main approaches are used: either adsorption of probe molecules or test reactions. Extensive studies have been devoted to characterizing the acidity of catalysts. Examples are pyridine adsorption (1) and low-temperature CO adsorption (2) studied by infrared spectroscopy and isopropanol dehydration as test reaction.

Basicity, on the other hand, has been studied to a lesser extent and is much more difficult to characterize (3). Isopropanol dehydrogenation is unsatisfactory in view of redox properties which interfere with the reaction (4). Recently, a new test reaction was proposed by Lauron-Pernot *et al.* (Scheme 1) (5): the conversion of 2-methyl-3-butyn-2-ol (methylbutynol, MBOH) giving acetone and acetylene on basic catalysts, or 3-methyl-3-buten-1-yne (MBYNE) with 3-methyl-2-buten-1-al (PRENAL) on acid catalysts. In addition to these products 3-hydroxy-3-methyl-2-butanone (HMB) and 3-methyl-3-buten-2-one (MIPK) can be formed, probably through the intervention of acid–base pairs.

This reactivity test using MBOH gives quite satisfactory results in the characterization of basic properties. A recent study (6) has shown this test to be independent of the nature of basic sites (Brønsted or Lewis) making it a global measure of basic properties. However, the mechanism of HMB formation is unknown and the hypothesis involving the intervention of acid–base pairs is unconfirmed. The aim of the present study is to specify the mechanisms and active sites in the case of zirconia which is very selective in HMB. ZrO_2 is a weakly acidic oxide, the type of acidity being mainly Lewis (7). The strength of Lewis acid sites can be estimated from the pyridine ν_{8a} band frequency (1607 cm^{-1}), much lower than those observed on Al_2O_3 (1622, 1617 cm^{-1}) and even on TiO_2 (1610 cm^{-1}) (8). The strength of basic sites

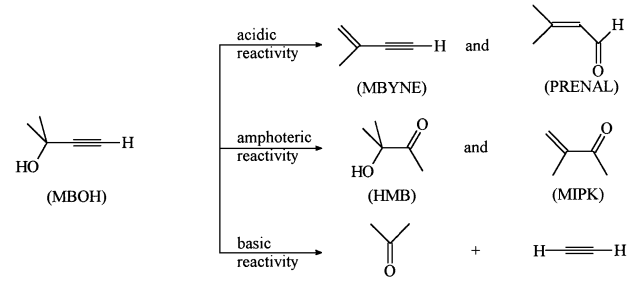

SCHEME 1. Overall reaction scheme. MBOH, 2-methyl-3-butyn-2-ol; MBYNE, 3-methyl-3-buten-1-yne; PRENAL, 3-methyl-2-buten-1-al; HMB, 3-hydroxy-3-methyl-2-butanone; MIPK, 3-methyl-3-buten-2-one.

[1] To whom correspondence should be addressed. Fax: 02 31 45 28 22. E-mail: LAVALLEY@ISMRA.UNICAEN.FR.

[2] Laboratoire de Réactivité de Surface et Structure, Université P. et M. Curie, Paris VI, Tour 54, 2ème étage 4, Place Jussieu, 75252 Paris Cedex 05, France.

[3] Rhône Poulenc, Centre de Recherches d'Aubervilliers, 52 Rue de la Haie Coq, 93308 Aubervilliers, France.

0021-9517/97 $25.00

is considered moderate as shown by CO_2 adsorption, and does not change much with the pretreatment temperature of the sample (7). High catalytic activities and selectivities of ZrO_2 for particular reactions have been explained involving the suitable orientation of the acid–base pair sites (7).

The main technique used for this study is dynamic *in situ* infrared spectroscopy, allowing the evolution of species to be monitored under conditions resembling those of the reaction. The bands are assigned to the corresponding vibration modes after complementary adsorption studies, in static mode, of the reactants and products of this reaction. The MBOH → HMB conversion formally being a hydration, we have specified the role of zirconia surface hydroxyl groups using more or less hydroxylated samples and studying the effect of adding water to the reaction mixture. The study is complemented by quantum chemistry calculations interpreted in mechanistic terms.

METHODS

Zirconia was prepared by hydrolysis of zirconium *n*-propylate and calcinated at 550°C (9). Its specific area is 70 $m^2\ g^{-1}$.

The MBOH used was from Fluka and contained 1.7 g/liter of water (about 1 mol%) as measured by the Karl–Fischer method. Acetone (99.8% Normapur) was from Prolabo, isophorone (98%) from Lancaster, and HMB (95%) from Janssen.

FT IR Experiments

In all experiments the catalyst was pressed into self-supporting discs of about 20 mg (10 mg cm^{-2}).

Flow experiments. The experiments under flow were carried out at atmospheric pressure using an infrared reaction cell (10). The catalyst was activated under nitrogen flow (15 $cm^3\ min^{-1}$) in the reactor cell at 400°C, the temperature being subsequently reduced to 180°C (reaction temperature) before introducing a flow of nitrogen (10 $cm^3\ min^{-1}$) carrying 4.45% MBOH via a saturator at 35°C in such a way as to obtain a partial pressure of 33.8 Torr (11) (1 Torr = 133.3 N m^{-2}). Monitoring the adsorbed species by infrared spectroscopy at the catalyst surface was carried out simultaneously using a Nicolet 5SX IR spectrometer. The exit gases from the reactor cell were analyzed using gas-phase chromatography with a Delsi chromatogram and Girdel 300 with a flame-ionization detector and a 50-m WCOT quartz capillary column (with CP sil 8 CB stationary phase). The first point on the conversion and selectivity curves was obtained after 4 min of reaction.

The results are expressed in terms of conversion and selectivity. C_i is the molar concentration of product i in the gas phase and $(C_{MBOH})_0$ is the initial molar concentration of MBOH. The conversion is expressed as

$$\text{conv}\% = \left[\frac{(C_{MBOH})_0 - C_{MBOH}}{(C_{MBOH})_0}\right] * 100$$

and the selectivity in product i can be written as

$$S_i = \frac{\alpha_i C_i}{\sum \alpha_i C_i} * 100,$$

where the factor α is 0.5 for acetone and acetylene and 1 for all other products in order to account for the MBOH splitting into one acetone and one acetylene molecule.

Static-mode experiments. The catalyst was activated for 2 h either at 650°C (dehydroxylated zirconia) or at 400°C (partially hydroxylated zirconia) in a secondary vacuum. The IR spectra were recorded at room temperature using a Fourier transform infrared spectrometer (either the Nicolet 710 or the Magna 750). Gas-phase spectra were always subtracted from those obtained. Unless otherwise stated, the experiments were carried out at room temperature. In general the spectra presented are those of the adsorbed species from which the activated catalyst spectrum has been removed (difference spectra).

Calculations of Interest in Mechanistic Studies from Wavefunctions and Potentials of Quantum Chemistry

Population analysis. The partial charges on atoms in a molecule were calculated by summing the squared coefficients of the atomic orbitals on the atom for the molecular orbitals occupied. This procedure is referred to as Mullican analysis. It leads to results which may differ substantially from isolated to adsorbed molecules. The main reason for this phenomenon is that obviously isolated molecules contain a whole number of electrons. Including the reactive-site atomic orbitals in the molecular orbital analysis for the whole of the supermolecule comprising the adsorbate-site orbitals introduces the possibility of partial charge transfer from the adsorbate molecule to the site. In this process the molecule may formally acquire a noninteger charge.

Adsorption calculations. From the molecular orbitals of the adsorbate–substrate supermolecule we obtained the self-consistent reaction field (SCRF) due to charge, dipole, and higher moments inducing image moments in a semi-infinite substrate initially taken to be periodic. This supermolecule is treated by local SCRF. This means it can be considered to be "cut out" of the bulk with no "dangling" bonds because they are replaced by localized orbitals. This adsorbate–substrate active-site supermolecule is then embedded in an electronic potential with the requisite behavior of the bulk. Twenty metal atoms ensure size consistence of physical properties but good results can be obtained with fewer (at least eight).

The perturbations due to these induced moments may be included directly in the electronic potential. This was calculated in matrix form by determining matrix elements of the appropriate Green's function on the LCAO basis of Slater-type orbitals at the semiempirical or ab initio level. The Fourier transform of this Green matrix perturbed by the interaction potential yields the density matrix. A final SCF cycle provides the molecular orbital coefficients for the perturbed LCAO.

The procedure summarized in the previous paragraph was implemented in the GEOMOS and STOP-GREEN program packages at the semiempirical and ab initio levels for STO bases. These packages are available from QCPE [584 (1989) and 667 (1996), respectively] (12, 13).

We used an original quantum chemistry approach based on an embedded cluster and the additivity of electronic potentials. This method has been used previously to corroborate and complement infrared material, providing information on reaction intermediates involved in various hydrolysis and hydration reaction mechanisms studied in this laboratory. (14).

The calculations were carried out using the in-house versions of the cited QCPE programs written in Fortran 90 by one of the present authors. The load module was about 40 MBytes running on an IBM RISC 6000-3BT with 64 MBytes RAM.

RESULTS AND DISCUSSION

(A) Study of the Reaction and Species Formed

MBOH conversion at 180°C on zirconia activated at 400°C is represented in Fig. 1. It does not exceed 7% after 4 min in the reactive flow and decreases rapidly with time down to a mere 2% after 90 min. Conversely, the selectivity is nearly constant, HMB being the major product (60–70%). In addition to acetone and acetylene, small quantities of MIPK are detected (5%). Only traces of MBYNE are observed.

IR study of MBOH and HMB adsorption at room temperature (in static mode). The spectrum of activated zirconia essentially presents two bands due to hydroxyl group stretch frequencies (residual groups). They are situated at 3763 and 3668 cm^{-1} and assigned to type I and II hydroxyl groups, respectively (9, 15, 16). Their intensity depends on the activation temperature (16) (Fig. 2); in particular they tend to disappear after activation at 650°C. We also note the presence of residual carbonates first characterized by a band at 1019 cm^{-1} and then by bands at 1545 and 1448 cm^{-1} (17, 18); their relative intensity varies according to the temperature of activation. Their high thermal stability and band wavenumbers indicate that they are polydentate or bulk species. Therefore their influence on the surface properties would be very weak.

In Fig. 3 we report the pure-liquid-phase spectra of the two compounds MBOH and HMB. Very few complete IR studies have been made on MBOH (19, 20); most publications concentrate only on the OH or C≡C–H vibrations (21–26). In pure liquid, these compounds are self-associated by bridging hydrogen bonds (27) as shown by the broad OH stretching bands around 3375 and 3460 cm^{-1} for MBOH and HMB, respectively. As expected, the MBOH spectrum presents bands characteristic of the acetylene moiety: ν(≡C–H) at 3300 cm^{-1}, ν(C≡C) at 2117 cm^{-1}, and a band at 1215 cm^{-1} which could be the 2δ(C≡C–H) overtone (28).

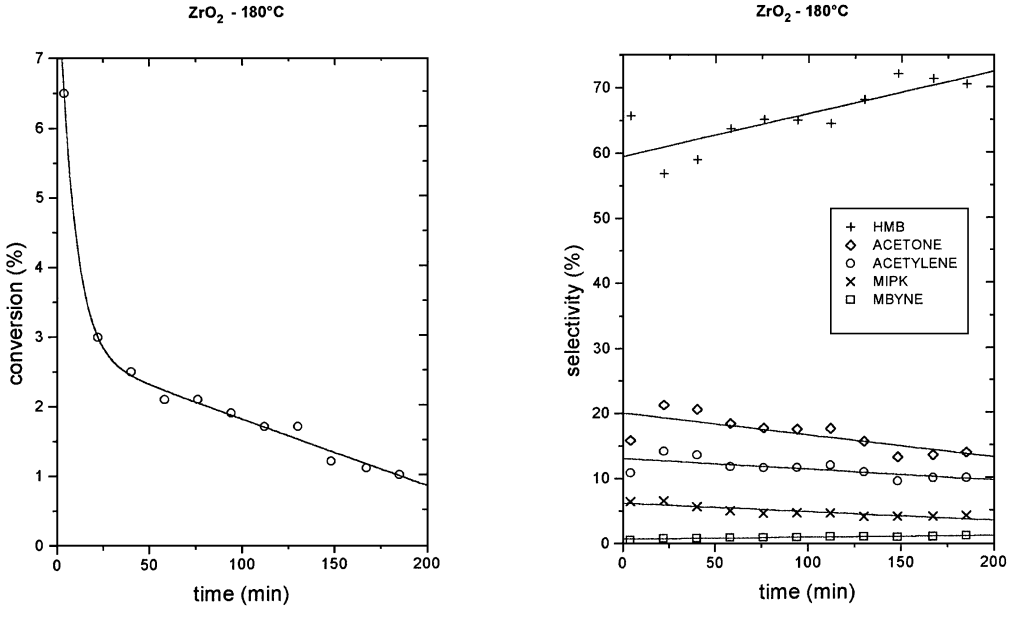

FIG. 1. Conversion and selectivity of MBOH at 180°C on ZrO_2 activated at 400°C for 1 h.

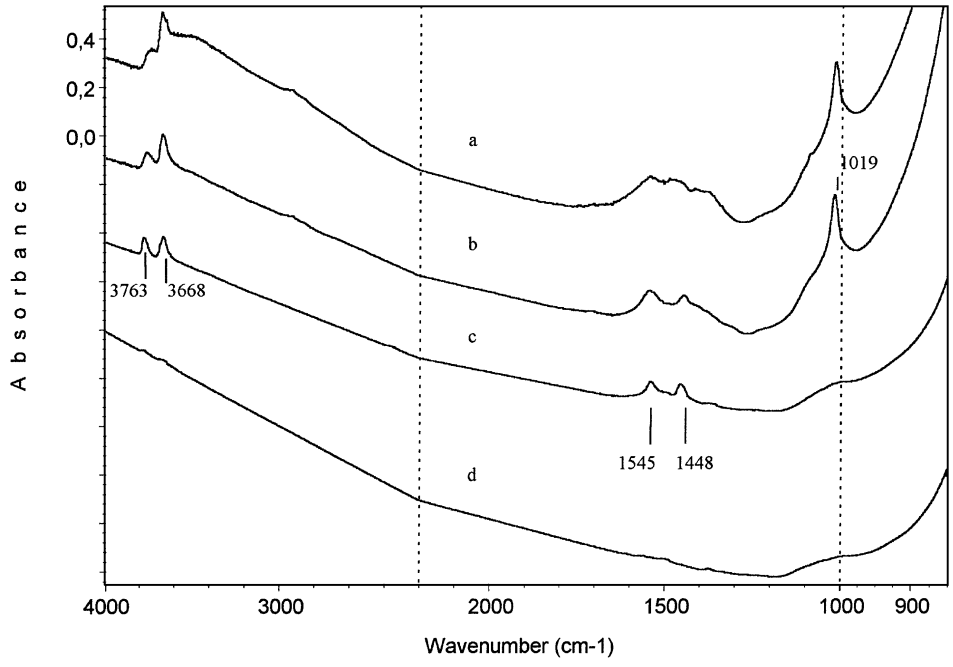

FIG. 2. IR spectra of ZrO_2 activated under different conditions: (a) 200°C under N_2 flow; (b) 400°C for 1 h and then return to 180°C under N_2 flow; (c) 400°C for 2 h in a vacuum; and (d) 650°C for 2 h in a vacuum.

The HMB liquid spectrum shows a very intense $\nu(C{=}O)$ band at about 1713 cm^{-1}. While the $\nu(CH_3)$ vibrations in the region 3000–2800 cm^{-1} are nearly identical, the two spectra (Fig. 3) are distinct for wavenumbers below 1500 cm^{-1}. Band assignment in this region is difficult because of vibrational couplings. It is possible to distinguish between the two compounds in the following manner: HMB gives a spectrum with extra bands at 1421 and 1130 cm^{-1} whereas the MBOH spectrum presents two sharp bands around 1215 and 889 cm^{-1}.

Figure 4a shows the spectrum of MBOH adsorbed on zirconia activated at 650°C (ZrO_2-650). It presents a ν(OH) band at 3540 cm^{-1} and a peak at 3318 cm^{-1} characteristic of the $\nu(\equiv C{-}H)$ band in the $C{\equiv}C{-}H$ group. The latter is

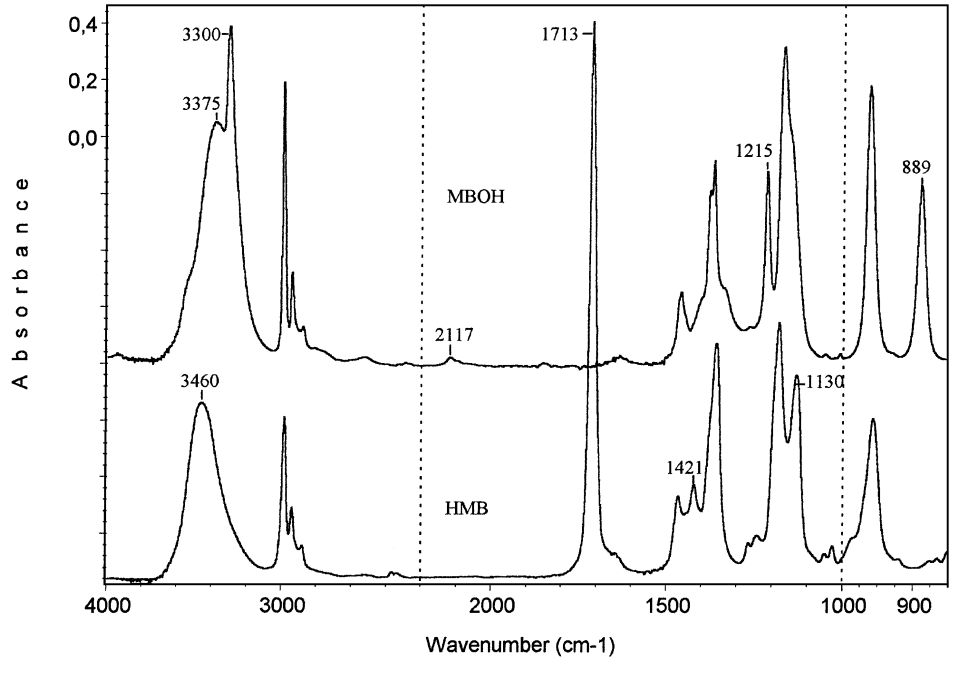

FIG. 3. Spectra of MBOH and HMB in the liquid state.

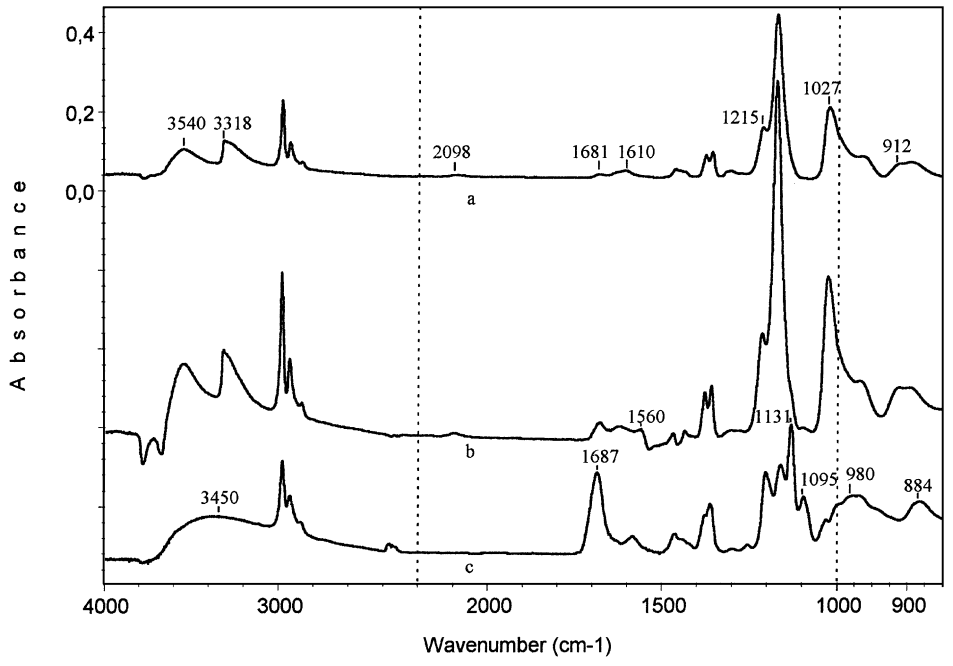

FIG. 4. IR spectra of species resulting from the adsorption of MBOH or HMB at room temperature on: (a) ZrO_2 activated at 650°C in a vacuum, 200 μmol g^{-1} MBOH; (b) ZrO_2 activated at 400°C for 2 h in a vacuum, 320 μmol g^{-1} MBOH; and (c) ZrO_2 activated at 650°C in a vacuum, 0.2 Torr HMB adsorbed at the equilibrium and then evacuated.

accompanied by a shoulder toward lower wavenumbers from 3300 to 3150 cm^{-1}. The ν(C≡C) band appears weak and very broad, its maximum at 2098 cm^{-1} being overlapped by a shoulder near ca. 2080 cm^{-1}. We also note the 2δ(C≡C–H) band near 1215 cm^{-1}. All these facts indicate that the C≡C–H group is perturbed but undissociated. We note two bands present at 1027 and 912 cm^{-1} which were absent from the MBOH liquid spectrum. These are assigned, by analogy to the results obtained from the study of tertiobutyl alcohol adsorbed on zirconia (17), to ν(C–O) and ν(C–C) vibrations in the alcoholate species. Formation of these species by *R*O–H bond breaking explains the presence of a broadband at 3540 cm^{-1} which resists evacuation and therefore does not correspond to physisorbed MBOH but to new hydroxyl groups formed:

$$Zr^{4+}\ O^{2-} \xrightarrow{ROH} \begin{matrix} & R & \\ & | & \\ Zr^{4+} & O & H \\ & | & | \\ & Zr^{4+} & O^{2-} \end{matrix} \qquad [1]$$

Note also two weak bands at 1681 cm^{-1} and 1610 cm^{-1}, the latter possibly resulting from the adsorption of water accompanying the MBOH. The 1681 cm^{-1} band is assigned, by comparison with the spectrum of adsorbed HMB (Fig. 4c) which presents a very intense band at 1687 cm^{-1}, to the C=O group of HMB-adsorbed species. Its presence indicates that the MBOH → HMB transformation has partly occurred at room temperature. Compared with the liquid HMB spectrum, we note in Fig. 4c the presence of new bands, in particular that at 1095 cm^{-1}, and the relative increase of the intensity of some others like that at 1131 cm^{-1}. They result from the coupling of the ν(C–O) and ν(C–C) vibrations. The occurrence of the new band at 1095 cm^{-1} tends to show that HMB is adsorbed in alcoholate form. The new OH groups formed by dissociative adsorption lead to a broadband at about 3450 cm^{-1} which resists evacuation at room temperature.

The effect of residual hydroxyls on the zirconia surface on the species formed by MBOH adsorption may be deduced by comparing the experiments carried out on zirconia activated at 400°C (ZrO_2-400) (Fig. 4b) and zirconia 650°C (ZrO_2-650) (Fig. 4a). Clearly, MBOH adsorbed on ZrO_2-400 perturbs the residual OH groups. The spectrum in the other regions is similar to that plotted in Fig. 4a showing the formation of alcoholate species. However, in the region 1700–1500 cm^{-1} we note the net intensity increase of the band at 1681 cm^{-1} showing HMB-adsorbed species formation to be favored and the appearance of a new band at 1560 cm^{-1}. We discuss the assignment of the latter in the acetone adsorption experiments presented below. The larger amount of HMB formed on ZrO_2-400 could result from the formation of additional water by MBOH condensation on the residual hydroxyls:

$$\begin{matrix} OH & H \\ | & | \\ Zr & O \end{matrix} + ROH \rightarrow \begin{matrix} OR & H \\ | & | \\ Zr & O \end{matrix} + H_2O \qquad [2]$$

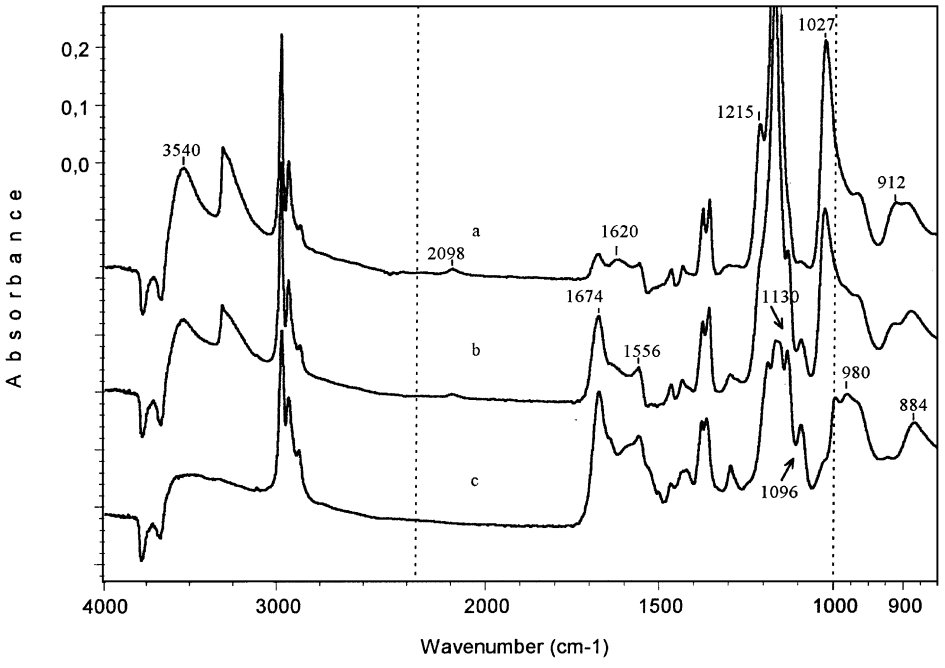

FIG. 5. IR spectra of species resulting from the adsorption of MBOH (320 μmol g^{-1}) at different temperatures on ZrO_2 activated in a vacuum for 2 h at 400°C: (a) at room temperature; (b) 3 min at 100°C; and (c) 5 min at 180°C.

The same type of reaction has been shown in the case of methanol adsorption at room temperature on zirconia preexchanged by $H_2{}^{18}O$ (17). This process explains the disappearance of the zirconia residual hydroxyls and its effect amplifies that described in Reaction [1], leading to alcoholate species with the same spectral characteristics.

Evolution of spectra with increase in temperature (static and under flow studies). We have studied the temperature evolution of the MBOH spectra on ZrO_2-400 (Fig. 5). We note that the bands due to residual free hydroxyls on the zirconia surface disappear whereas no band due to free hydroxyls reappears over the entire temperature range. The ν(OH) band at 3540 cm^{-1} resulting from dissociative adsorption of MBOH tends to disappear. The same is observed for bands characteristic of the C≡CH group (around 3300 and 2098 cm^{-1}) and those characteristic of the methylbutynolate species (at 1027 and 912 cm^{-1}). Concomitantly, the bands corresponding to HMB formed (1674, 1130, and 1096 cm^{-1}) increase in intensity. Below 1000 cm^{-1}, we find bands at 980 and 884 cm^{-1} also observed in the spectrum of adsorbed HMB (Fig. 4c) which confirm that this product is formed. Finally, in the region 1650–1500 cm^{-1}, heating leads to the disappearance of the band at 1620 cm^{-1} and to the corresponding appearance of that at 1556 cm^{-1}. These bands show that other species form on heating, the nature and role of which we will specify by flow experiments.

Spectra obtained in a flow of MBOH at 180°C are plotted in Fig. 6. We note the same tendencies as those observed in static mode at 180°C: the appearance of adsorbed HMB (1679, 1131, and 1094 cm^{-1}), the disappearance of the residual OH groups on zirconia, the absence of the band at 3540 cm^{-1}, and the appearance of two bands at least around 1620 and 1550 cm^{-1}. With time, the intensity of the ν(C=O) band at 1679 cm^{-1} decreases, corresponding to a decrease in activity of the catalyst as shown in Fig. 1. There is a parallel increase in the broadband at 1600–1550 cm^{-1}. Its origin was determined by experiments in an acetone flow at 180°C (Fig. 7). We first observe two ν(C=O) bands at 1688 and 1619 cm^{-1} assigned respectively to the adsorption of acetone and oligomers of mesityl oxide or isophorone type as shown by the adsorption of isophorone in flow (Fig. 7c). Also Zhang *et al.* observed aldolization followed by dehydration by introducing acetone on zirconia at 0°C (29). With time, the band intensity at 1688 cm^{-1} decreases and that at 1619 cm^{-1} increases and then decreases, leading to a new band at about 1560–1550 cm^{-1} due to acetone polymerization. No band due to free hydroxyls reappears for the entire duration of the MBOH reaction. These results are correlated with the decrease in catalyst activity with time (Fig. 1) and suggest that the sites are poisoned by species resulting from acetone polymerization.

(B) Effect of Water Addition

The transformation of MBOH species adsorbed into HMB species corresponds to the hydration of the triple bond. It requires the intervention of hydroxyl groups and/or water. In the previous experiments at 180°C we note the disappearance of the zirconia hydroxyl groups as soon as

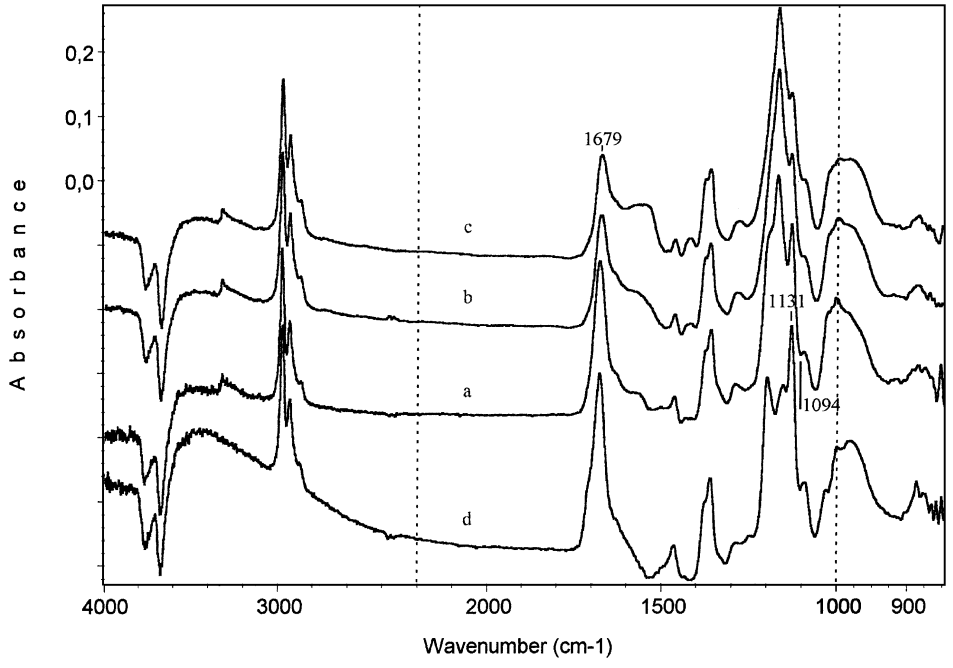

FIG. 6. IR spectra of species resulting from the adsorption of MBOH and HMB at 180°C on ZrO_2 activated under N_2 flow for 1 h at 400°C, at different times on flow. MBOH: (a) 44 s; (b) 30 min; (c) 2 h 10 min. HMB: (d) 124 s.

MBOH is added and also the absence of the ν(OH) band at 3540 cm^{-1} resulting from dissociative adsorption of MBOH. These hydroxyl groups can take part in the hydration of MBOH. In addition small amounts of water contaminate the reactant or result from acetone polymerization. The following experiments aimed to study the role of water introduced in the gas phase. For this purpose we added water to the liquid MBOH (0.4 mol H_2O/mol MBOH). The reactivity results are presented in Fig. 8. Note that the initial conversion is about five times greater than that observed in Fig. 1 but that the deactivation with reaction time persists. Selectivity in HMB is excellent (between 93 and 96%).

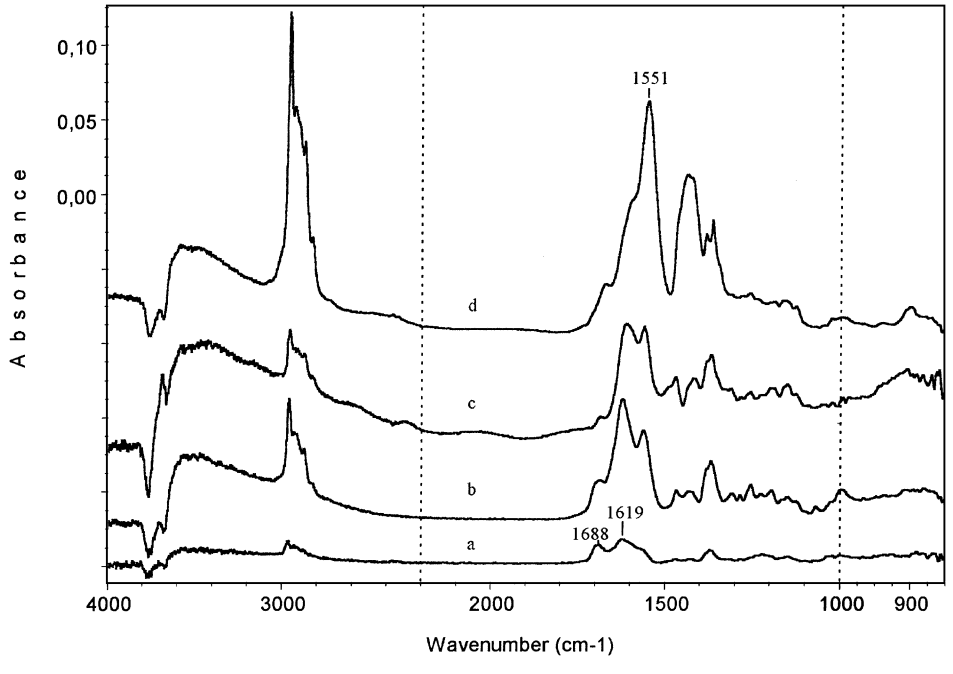

FIG. 7. IR spectra of species resulting from the adsorption of acetone and isophorone at 180°C on ZrO_2 activated for 1 h under N_2 flow at 400°C, at different times on flow. Acetone: (a) 22 s; (b) 48 s; (d) 45 min. Isophorone: (c) 38 min.

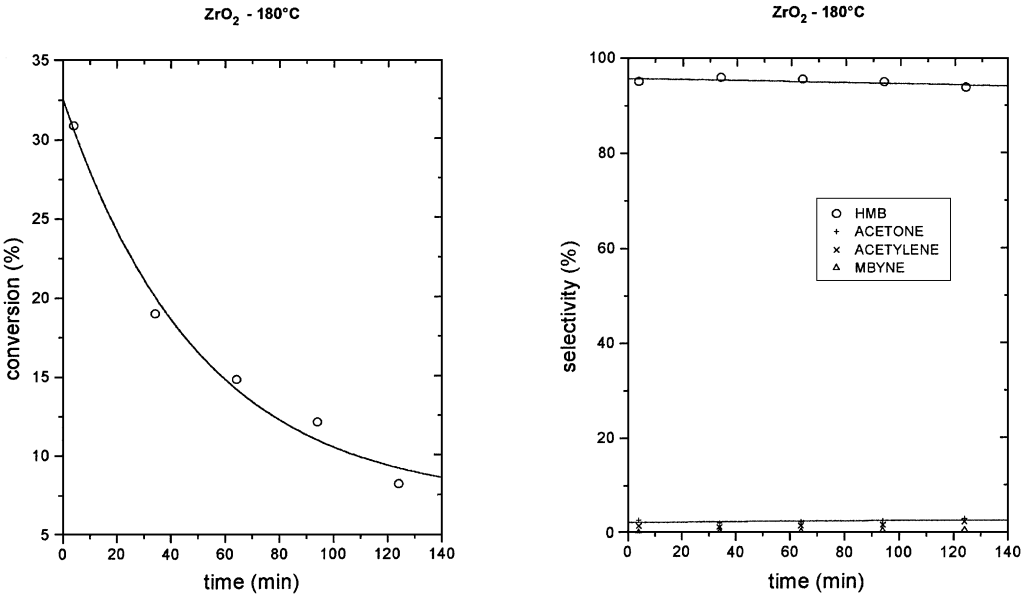

FIG. 8. Conversion and selectivity obtained under MBOH + H_2O flow at 180°C, on ZrO_2 activated at 400°C for 1 h.

However, in view of the strong initial conversion of the catalyst under these conditions, the quantities of acetone and acetylene formed are identical to those observed without additional water.

The dynamic monitoring of the reaction by infrared spectroscopy (Fig. 9) shows the consumption of zirconia surface hydroxyl groups. Very few adsorbed MBOH species appear [weak band at 3327 cm^{-1}, $\nu(\equiv C-H)$], the main bands observed (1674, 1132, 1092, 981, and 882 cm^{-1}) being due to HMB species adsorbed as alcoholates. As previously (Fig. 6) we note that the amount of HMB adsorbed decreases with time and can be explained by the polymerization of acetone (band at 1550 cm^{-1} with intensity increasing with time). It has also been reported in the literature that water addition favors polymerization on MgO (29). These results show that the rate of MBOH conversion into HMB

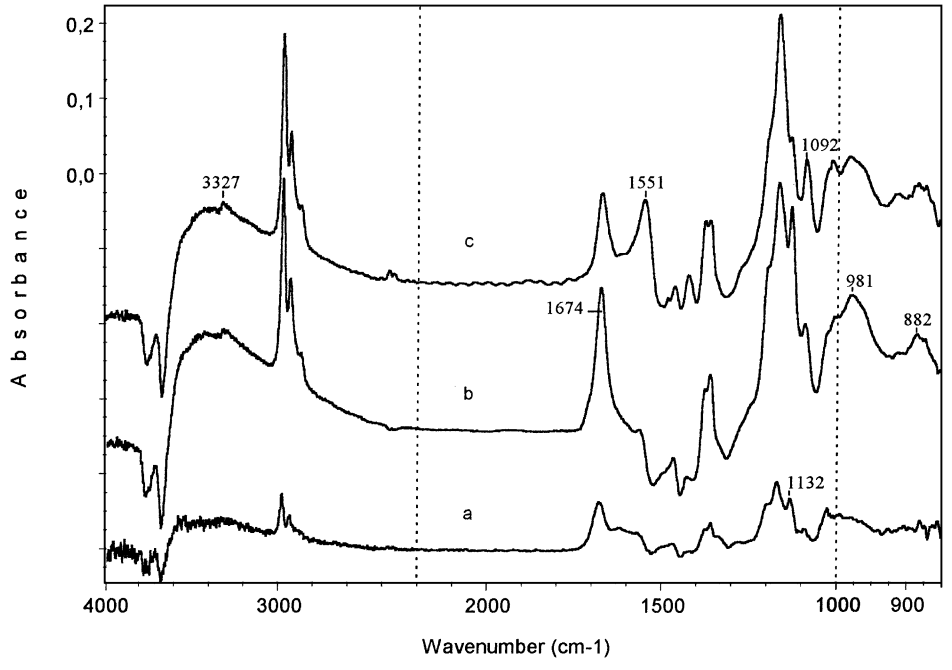

FIG. 9. IR spectra of species resulting from MBOH + H_2O adsorption at 180°C on ZrO_2 activated at 400°C for 1 h under N_2 flow, at different times on flow. (a) 16 s; (b) 10 min; (c) 2 h 17 min.

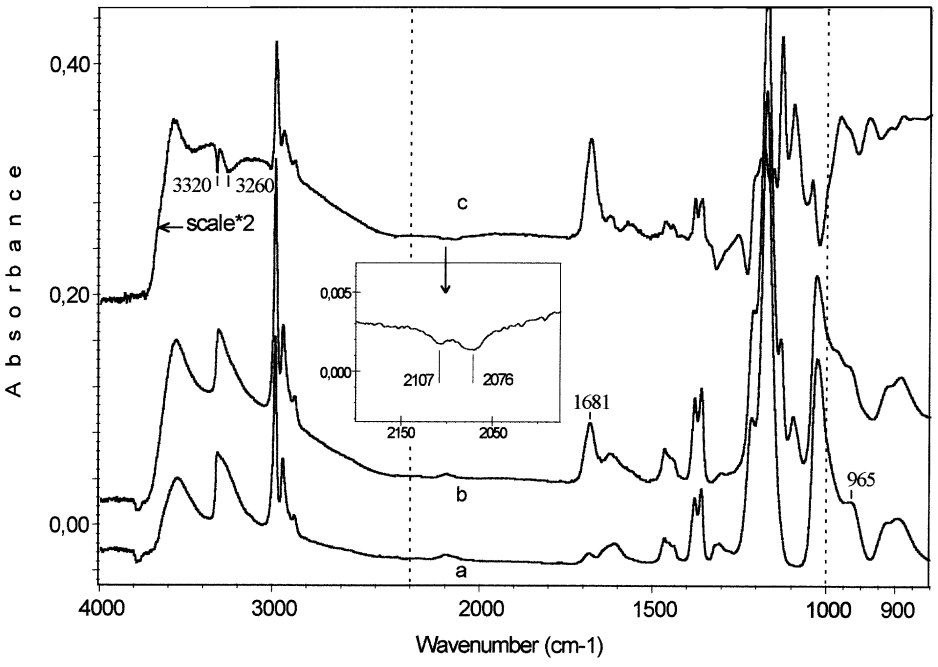

FIG. 10. Effect of the addition of water on the spectra of species resulting from MBOH adsorption on ZrO_2 activated at 650°C. (a) 200 μmol g^{-1} MBOH; (b) addition of 100 μmol g^{-1} H_2O; (c) = b − a.

is greatly increased by the introduction of water in the gas phase. Conversely, such water addition leaves the conversion to acetone and acetylene unaffected and thus will not interfere with the detection of zirconia basic properties.

The flow experiments show that the reactivity of the C≡C−H group is too great to allow its activation to be studied. The hydration mechanism was therefore studied in static mode at room temperature.

Approaching the reaction mechanism. In an experiment (Fig. 10a) MBOH (200 μmol g^{-1}) was introduced at room temperature onto zirconia activated at 650°C. This temperature was chosen to ensure that very few residual hydroxyls are present. The species formed are chiefly MBOH adsorbed in the form of alcoholates. The addition of water (100 μmol g^{-1}) at room temperature noticeably increases the band intensity characteristic of adsorbed HMB (1681 cm^{-1}) (Fig. 10b): the intensity is about a quarter of that obtained by saturation of the ZrO_2 surface with HMB (Fig. 4c). It shows that a substantial amount of HMB can be formed by hydration of MBOH adsorbed as alcoholate species on Zr^{4+} O^{2-} pair sites as confirmed by the concomitant appearance of HMB species and the disappearance of the MBOH alcoholate species. The difference spectrum, obtained by subtracting that recorded before adding water, allows us to specify which C≡C−H groups have disappeared (Fig. 10c). Regarding the ν(≡C−H) region, two "negative" bands are noted, a sharp one at 3320 cm^{-1} corresponding to a free ≡C−H group and the other band at around 3260 cm^{-1} due to a perturbed ≡C−H group. In the ν(C≡C) region two bands have also decreased in intensity, one at 2107 cm^{-1} and the other at 2076 cm^{-1}.

Physisorbed MBOH species cannot be excluded in the spectrum obtained after introducing 200 μmol g^{-1} MBOH; they would explain the sharp band at 3320 cm^{-1} and that at 2107 cm^{-1}, ν(C≡C) (such a hypothesis being confirmed by the observation of a shoulder at 965 cm^{-1}). These species would be displaced by the introduction of water. As regards ν(C≡C) and ν(≡C−H) bands at 2076 and 3260 cm^{-1}, respectively, they could be indicative of an MBOH species with a perturbed C≡C−H group possibly interacting with a zirconium atom, as the quantum chemistry results below suggest and which would facilitate the hydration.

(C) Quantum Chemistry Viewpoint

The hydration process is believed to proceed via an initial nucleophilic attack on the *sp* hybridized carbon atom with the largest partial positive charge (obtained by calculating Mullican population analyses over the molecular orbitals, see Methods). For the free MBOH molecule, the greatest partial positive charge would be the terminal carbon atom (Fig. 11a). With such a polarization, we would expect to obtain the corresponding aldehyde. MBOH adsorption in the form of its alcoholate species does not reverse the C≡C polarity, as shown in Fig. 11b involving an adsorbate-site supermolecule including 20 atoms of the zirconia surface. A further interaction must be involved to provoke the charge redistribution and the reverse C≡C polarity. This interaction directly transfers charge from the carbon $2p_z$ orbital

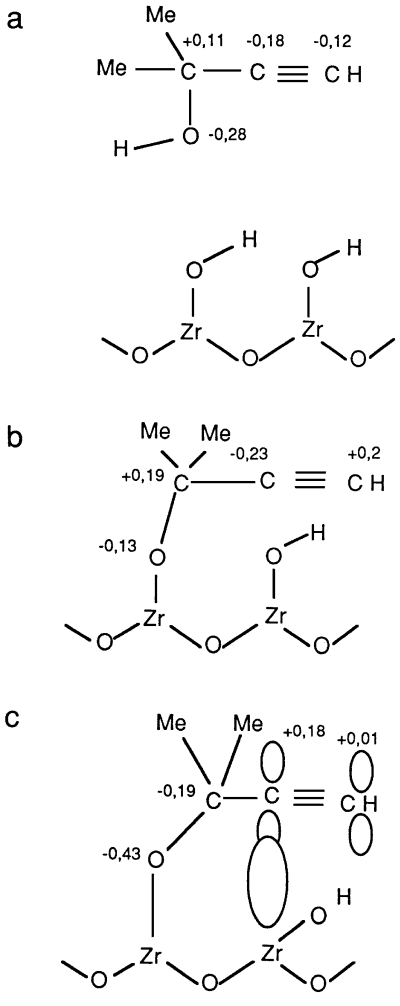

FIG. 11. Activated complex structures illustrating the three steps of MBOH alcoholate formation on a zirconia surface. The diagrams show a slice through the zirconia surface. The zirconium atoms are in fact hexacoordinated in this case. (a) Physisorption-activated complex; (b) alcoholate formation intermediate; and (c) specific interaction between acetylenic π-bond and vacant zirconium *d*-orbital transition state.

involved in the triple C≡C bond (C≡C−H) to a vacant zirconium *d* orbital. The nucleophilic attack by a basic hydroxyl group, already bound to the surface or resulting from water dissociation, is followed by a proton attack, and first leads to an enol which then isomerizes into the ketone form (HMB).

Quantum calculations provide clear geometric insight into the mechanism operating on a fully hydrated zirconia surface.

Zirconia involves zirconium atoms, each of which has two occupied *d* orbitals which belong to the E representation that is energetically stabilized in an environment of T_d (tetrahedral) symmetry, close to that assumed for the bulk periodic structure (30). The *d* orbitals in question are those labeled $4d_{z^2}$ and $4d_{x^2-y^2}$. They are directed between the tetrahedral axes and therefore minimally affected by the electronic repulsion due to the apical oxygen atoms. Three vacant *d* orbitals remain. They are those labeled $4d_{xy}$, $4d_{yz}$, and $4d_{xz}$. Their positions are such that the lobes are directed at 45° from the previous (occupied atomic *d* orbitals) and they constitute a basis for the T_2 representation of the tetrahedral group. The fact that they are vacant in the bulk lattice minimizes possible repulsion due to the electrons of the oxygens because they are quite close to (and in one case exactly directed in) the directions of these oxygen atoms in the bulk lattice. However, as far as the surface atoms are concerned, the situation is quite specific, since the $4d_{x^2-y^2}$ orbital participates in the Zr−OH bond and therefore the $4d_{yz}$ must be in the direction of the C≡C−H methylbutynol carbon atom once the methylbutynol molecule has been coordinated to the surface by the attack of a hydroxyl group on the zirconium atom (Figs. 11a and 11b). This vacant zirconium *d* orbital also possesses the appropriate symmetry (in particular phase) to generate an efficient overlap with the $2p_z$ orbital on the C≡C−H carbon atom. The phase of an orbital is its sign in a given region of space. For good overlap and hence bonding interaction, orbitals should have the same sign between the atoms concerned, as in the present case. The carbon 2*p* orbital involved is specifically the one which characterizes the difference between the hybrids before and after nucleophilic attack and proton transfer.

Clearly therefore, it is possible to determine the charge transfer which proves to be largely specific to the atomic orbitals cited, on the basis of LCAO coefficients calculated in the course of the reaction, visualized as advancing along the reaction coordinate by geometry optimization procedures which we carried out at the semiempirical level using the author's MNDO2 Hamiltonian and parameter sets for the second-row transition metals (31). The transfer amounts to 28% (Fig. 11c) of an electronic charge which is quite spectacular and greatly catalyzes this reaction with high specificity in the selective yield of the hydration product.

CONCLUSION

The zirconia active sites have been considered weak acidic–moderately basic pair sites (7). The MBOH test confirms that ZrO_2 acidity is very weak since a very small amount of MBYNE and the absence of prenal are observed. As for ZrO_2 basicity, the amount of acetylene and acetone formed (Fig. 1) shows that it is not as strong as that observed on MgO, for instance (5). Moreover, it does not vary with the addition of water, confirming that it is independent of the nature (Brønsted or Lewis) of basic sites (6).

The present study also shows that MBOH conversion to HMB proceeds via transformation of alcoholate species (resulting from dissociative MBOH adsorption). The sites involved are Zr−O pairs of hydroxylated Zr−O pairs which trigger an acetylenic π electron–vacant zirconium *d*-orbital interaction in addition to the dissociative adsorption of MBOH. Water being a reactant for HMB formation, it

should be added to MBOH flow to ensure significant activity, and thus good detection of this kind of site when presumed on the catalyst tested.

Current studies show that TiO_2 also induces a MBOH → HMB transformation, enhanced by the addition of water. Again an interaction between the acetylenic π electrons and vacant titanium *d* orbitals could be involved which tends to generalize the present results.

REFERENCES

1. Parry, E. P., *J. Catal.* **2**, 371 (1963).
2. Zaki, M. I., and Knözinger, H., *Spectrochim. Acta A* **43**, 1455 (1987).
3. Lavalley, J. C., *Catal. Today* **27**, 377 (1996).
4. Lahousse, C., Bachelier, J., Lavalley, J. C., Lauron-Pernot, H., and Le Govic, A. M., *J. Mol. Catal.* **87**, 329 (1994).
5. Lauron-Pernot, H., Luck, F., and Popa, J. M., *Appl. Catal.* **78**, 213 (1991).
6. Huang, M., and Kaliaguine, S., *Catal. Lett.* **18**, 373 (1993).
7. Tanabe, K., *Mater. Chem. Phys.* **13**, 347 (1985).
8. Lahousse, C., Aboulayt, A., Mauge, F., Bachelier, J., and Lavalley, J. C., *J. Mol. Catal.* **84**, 283 (1993).
9. Aboulayt, A., Binet, C., and Lavalley, J. C., *J. Chem. Soc. Faraday Trans.* **91**, 2913 (1995).
10. Joly, J. F., Zanier-Szydlowski, N., Colin, S., Raatz, F., Saussey, J., and Lavalley, J. C., *Catal. Today* **9**, 31 (1991).
11. Conner, A. Z., Elving, P. J., Benischeck, J., Tobias, P. E., and Steingiser, S., *Ind. Eng. Chem.* **42**, 106 (1950).
12. Rinaldi, D., Hoggan, P. E., and Cartier, A., GEOMOS package, QCPE 584 (1989).
13. Bouferguene, A., and Hoggan, P. E., STOP, QCPE 667 (1996).
14. Hoggan, P. E., Bensitel, M., and Lavalley, J. C., *J. Mol. Struct.* **320**, 49 (1994) and references therein.
15. Yamaguchi, T., Nakano, Y., and Tanabe, K., *Bull. Chem. Soc. Jpn.* **51**, 2482 (1978).
16. Bensitel, M., Moravek, V., Lamotte, J., Saur, O., and Lavalley, J. C., *Spectrochim. Acta A* **43**, 1487 (1987).
17. Bensitel, M., Ph. thesis, Caen, France, 1988.
18. Busca, G., and Lorenzelli, V., *Mater. Chem.* **7**, 89 (1982).
19. Zyat'kov, I. P., Ol'dekop, Yu. A., Yuvchenko, A. P., Ksenofontova, N. M., Pitsevich, G. A., Sagaidak, D. I., Gogolinskii, V. I., and Antonovskii, V. L., *Zh. Prikl. Spektrosc.* **48**, 585 (1988).
20. Kharitonov, Yu. Ya., Beresneva, T. I., Mazo, G. Ya., and Babaeva, A. V., *Russ. J. Inorg. Chem.* **13**, 1129 (1968).
21. Singelenberg, F. A. J., Visser, T., and van der Maas, J. H., *J. Mol. Struct.* **175**, 239 (1988).
22. Visser, T., and van der Maas, J. H., *Spectrochim, Acta A* **40**, 959 (1984).
23. Visser, T., and van der Maas, J. H., *Spectrochim. Acta A* **39**, 241 (1983).
24. Kruglikova, R. I., and Porotnikova, A. I., *Zh. Org. Khim.* **13**, 1355 (1977).
25. Lutskii, A. E., Shuster, Ya. A., Granzhan, V. A., and Zaitsev, P. M., *Zh. Prikl. Spektrosc.* **16**, 870 (1972).
26. Nyquist, R. A., and Potts, W. J., *Spectrochim. Acta* **16**, 419 (1960).
27. Cabanetos, M., and Wojtkowiak, B., *C. R. Acad. Sci. Paris C* **268**, 751 (1969).
28. Saussey, J., Ph. thesis, Caen, France, 1978.
29. Zhang, G., Hattori, H., and Tanabe, K., *Appl. Catal.* **36**, 189 (1988).
30. Mc Dermott, T. E., *Coord. Chem. Rev.* **11**, 1 (1973).
31. Hoggan, P. E., and Rinaldi, D., *Theor. Chim. Acta* **72**, 467 (1987).